

Full VNIR-SWIR hyperspectral imaging workflow for the monitoring of archaeological textiles

Federico Grillini¹, Jean-Baptiste Thomas^{1,2}, Sony George¹.

¹ Department of Computer Science – Norwegian University of Science and Technology; Gjøvik, Norway.

² ImViA Laboratory - University of Burgundy; Dijon, France.

Abstract

A practical workflow to capture and process hyperspectral images in combined VNIR-SWIR ranges is presented and discussed. The pipeline demonstration is intended to increase the visibility of the possibilities that advanced hyperspectral imaging techniques can bring to the study of archaeological textiles. Emphasis is placed on the fusion of data from two hyperspectral devices. Every aspect of the pipeline is analyzed, from the practical and optimal implementation of the imaging setup to the choices and decisions that can be made during the data processing steps. The workflow is demonstrated on an archaeological textile belonging to the Paracas Culture (Peru, 200 BC - 100 AD ca.) and displays an example in which an inappropriate selection of the processing steps can lead to a misinterpretation of the hyperspectral data.

Introduction

Textiles are sometimes one of the few pieces of evidence left by ancient civilizations, and their study and preservation can allow speculation about the beliefs, traditions, and technological advances of their original manufacturers.

The first evidence of textile artefacts dates back around the year 8000 BC and is attributed to early civilizations in the Peruvian Andes [1]. As time progressed, the subsequent cultures started to forage different types of fibers based on the local availability of flora and fauna; and started engineering novel manufacturing processes that over the years saw the development of advanced looms, tapestries, and embroideries. Technological advances also concern the artistic and aesthetic sides of textile creation: discovering specific dyestuff and mordants in an artefact can result in great insights about the knowledge gained by a civilization on extraction and synthesizing processes.

Broadly speaking, a textile can be summarized as an organized weaving structure constituted of warps and wefts, in which potentially different fibers are colored by one or more dyes thanks to mordants acting as binding agents. The presence of numerous compounds, at times both organic and inorganic, requires specific analytical tools in order to be able to characterize the different components. Fibers can be identified for example by means of Raman, optical, and Fourier transform-based spectroscopy techniques [2, 3, 4]. X-Ray Fluorescence can be deployed to characterize mordants [5], while various techniques such as liquid chromatography coupled with diode array detector (HPLC-DAD) and Surface Enhanced Raman Spectroscopy (SERS) can help in discriminating between different dyes [6, 7].

Although very accurate, most of the aforementioned techniques require either the irreversible extraction of samples from the textiles or the exposure of the artefacts to potentially harmful radiation that can denature the chemical bonds.

Imaging, on the other hand, is a completely non-invasive

technique that can aid archivists and conservation scientists in carrying out monitoring and analytical tasks. High-resolution imaging can be easily accessed in those spectral ranges with low radiating energy (longer wavelengths) in which textiles often exhibit particular features regarding their material composition: visible light (from 400 nm to 700 nm) can help in discerning different dyes [8], while it has been found that different fibers are prone to present characteristic features when exposed to infrared radiation [9].

Reflectance imaging spectroscopy, also known as hyperspectral imaging [10], is particularly suitable to analyze archaeological textiles since it privileges objects with a rather flat surface. The result of hyperspectral imaging is an *image cube* constituted by a stack of N image planes each relative to a specific wavelength. If a pixel is investigated individually, it will be described by a series of N values that compose its spectral profile, or spectrum. When carefully calibrated, the pixel values can be transformed to represent physically meaningful quantities such as radiance, reflectance, transmittance, and absorbance.

What limits the spectral range of a hyperspectral system is usually the material with which the sensor is manufactured, therefore the solution adopted to explore a wider range is normally to deploy multiple sensors. Two sensors can usually cover the range from the visible (VIS) through the near-infrared (NIR) and the short-wave infrared (SWIR).

The study of textiles by means of hyperspectral imaging has been conducted on various occasions [11, 12]. However, it is noticeable that whenever two modalities of imaging are deployed (visible and infrared), the two datasets are often treated independently rather than in a combined fashion. In this instance, there is no synergy and *cross-talk* between the two types of information. We argue that the term *cross-talk* is used here in its positive meaning: when two datasets are allowed to interact, it is possible that new features are created, and such features can be exploited to highlight similarity or dissimilarity patterns that can be otherwise lost. In terms of monitoring, it is also more useful to have a single image cube that spans the whole spectral range in which the information at the pixel level is precisely aligned.

In this article, which wants to serve as a demo for conservation and archival practitioners, we explore how to merge the information from two different hyperspectral datasets acquired in the Visible and Near-Infrared range (400 – 1000 nm) and the SWIR range (1000 – 2500 nm). The discussion will focus on considerations of how to build the most optimal imaging set-up, data fusion at the spatial and spectral levels, and data enhancement. Regarding the last point, we demonstrate how the selection of a sub-appropriate enhancement technique can lead to errors in the classification of textile fibers.



Figure 1. Fragment UEM37917 belonging to the small collection of Paracas textiles. **a)** Full composite image that results from the alignment of the individual scans (1 and 2) in **b)**. All figures are rendered to sRGB from reflectance data, assuming the CIE (International Commission on Illumination) D_{65} standard illuminant and 2° standard observer.

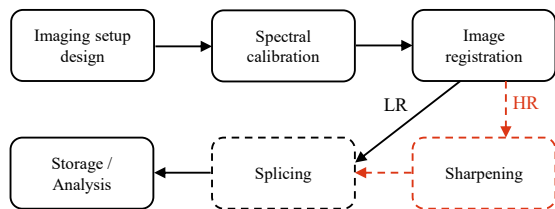


Figure 2. Workflow for the acquisition and processing of hyperspectral images in combined VNIR-SWIR. LR in black: workflow steps at low spatial resolution. HR in red: workflow steps at high spatial resolution..

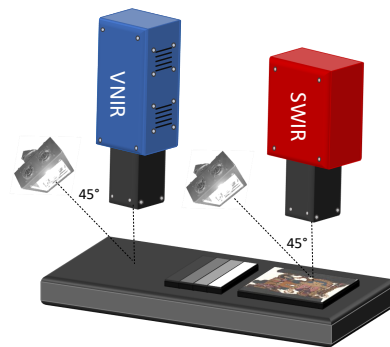


Figure 3. Experimental set-up. The cameras are placed side by side, while the relative angles between the target, illumination, and viewing direction must be kept as similar as possible between the two independent systems.

Materials

The selected case study is a textile fragment (ID: UEM37917) belonging to a small collection of Paracas textiles housed at the Museum of Cultural History of the University of Oslo, Norway. The fragment, depicted in Figure 1a, is dated to the period 200 BC – 100 AD, and given its age, the fibers have been consumed by erosion, while colors still appear somewhat vibrant. This quite good state of preservation can be attributed to the dry climate of the Peruvian desert. The dimensions of the fragment are 23 x 20.5 cm. To capture hyperspectral images, two push-broom (line scanner) cameras developed by Hypspec (Norsk Elektro Optikk, Norway) have been deployed. The VNIR camera operates in the spectral range from 400 to 1000 nm with a Silicon-based sensor (CMOS), yielding 186 bands with a spatial resolution of 1800 pixels on the acquisition line. The SWIR camera deploys a Mercury-Cadmium-Telluride sensor that captures radiation from 950 to 2500 nm (288 bands), while its spatial resolution is only 384 pixels on the acquisition line. The gap in spatial resolution, which translates to a ground sampling distance (GSD) of about $50\mu\text{m}$ for VNIR against $200\mu\text{m}$ for SWIR, poses a first problem in image alignment.

Workflow Overview

The workflow followed in this article for the capturing and processing of VNIR-SWIR hyperspectral data of archaeological textiles is illustrated in Figure 2. We shall define each step in the present section, while the next section will feature a discussion about specifics and links between the blocks of the workflow.

An accurately designed experimental set-up has a three-fold

purpose: firstly, it must prevent any harm to the studied artefacts, then it should allow the acquisition of high-quality data, and finally, it should facilitate the later processing steps. A schematic depiction of the adopted set-up is reported in Figure 3.

By **spectral calibration**, it is intended the series of processing steps that transforms the data from RAW values to calibrated reflectance values. After the first step of radiometric correction, in which the influence of camera and user-dependent parameters are discarded, the standardized target (Spectralon – LabSphere) is used to perform flat field correction - in which the heterogeneity of the light field is corrected - and normalize data from relative radiance to reflectance.

The goal of **image registration** [13] is to align a pair of images acquired in different conditions, e.g. image modality or viewpoint. One of the two images is selected as the *reference* (or fixed) image, while the other will be the *target* (or moving) image. Most image registration methods rely on the identification and matching of specific spatial structures such as corners and edges between the reference and target images, or on the maximization of similarity between the image pair. Once the matching features are identified, a mathematical transform (homography) is learned and applied to the target image.

Splicing [14] is a spectral correction that is applied whenever two sensors capture information in adjacent or overlapping spectral ranges. What is normally observed at these particular

wavelengths is a mismatch in values of the order of 1 – 5%. The correction aims at modifying, without denaturing, the spectra so that they form a smooth continuous spectrum in a wide spectral range.

What has been presented so far allows to generate a combined spectral cube with bands spanning from 400 to 2500 nm, at the lower available resolution, i.e. that of the SWIR camera. This is the workflow reported in Figure 2 in black.

But what if the goal is to obtain the same cube at the highest sensor resolution? In order to do so, it is necessary to add a step of *sharpening* between the spatial registration and spectral splicing steps (red workflow in Figure 2).

Image sharpening techniques, developed first in the field of remote sensing [15], enhance the spatial resolution of a target image. The vast majority of sharpening techniques rely on the presence of a reference image of higher resolution that usually guides the enhancement. In *Pansharpening*, the spatial details of a panchromatic (gray level) image are injected onto a multiband image of lower resolution. In *Hypersharpening* [16], like in our case, the guiding image is a hyperspectral set.

In general, sharpening techniques suffer from a major evaluation issue, since the ground truth of the enhanced image is never available. For this reason, the evaluation is generally carried out following Wald's protocol [17]. Here, the two image sets are degraded in resolution, so that the originally captured image can be deployed as ground truth. Wald's protocol implicitly assumes that the sharpening methods are scale-invariant, i.e. their performances do not change when the resolution of the image content is increased/decreased.

Lastly, it is important to point out that sharpening comes also at the cost of management. Computational power and storage resources are proportional to the size of the image to be sharpened, and an image cube with hundreds of bands at high spatial resolution will have a size on disk of several gigabytes (often more than 10). Strategies of lossless compression should be carefully examined in order to have more sustainable storage and faster access, but this is outside the scope of the current article.

From general to specific

In this section, we shall discuss more in detail the steps presented in the workflow and look into how practical decisions adopted in the designing of the imaging setup can positively influence the success of the later steps.

Starting from artefacts prevention, although reflectance imaging spectroscopy is considered a fully non-invasive technique, it can still pose a few risks to the textiles. Infrared radiation, by nature, causes the receiving medium to heat up, and therefore the exposure must be controlled so that only the smallest number of illumination sources that allow to capture high-quality data are used. In our setup, a single halogen light is deployed per camera. The generated light fields reach a maximum illuminance of 25000 lux concentrated on a narrow line aligned with the acquisition lines of the cameras. Given the adopted integration time of 20 μ s, we estimate that each pixel receives an exposure of approximately 91 klux during the 4 minutes in which the artefact is scanned. This value is reportedly acceptable [18] since it does not provoke significant spectral variations on the textiles. To put the estimated digit in perspective, one scan corresponds to exposing the artefact to solar light (10klux) for about ten seconds, or 114 days of exhibition (8 hours per day) in a museum at 100 lux of illuminance.

Having good image quality normally boils down to achieve

a high signal-to-noise ratio (SNR) and to generate visually pleasing images. In spectral imaging, the concept of image quality can be extended to include concepts of spectral fidelity, for which it is expected to observe smooth spectral profiles from natural materials. Possibly, a definition of a *good* spectral image can be a spatially sharp image content with smooth spectral features.

Achieving the maximum spatial quality can be beneficial also to improve registration since it will be easier to identify the anchor points that are used to learn the transformation between the two images. Another beneficial factor for image registration is a high content overlap, which can be achieved by aligning the two imaging systems. It must be said that in instances of cameras with fixed focus distances and different angular apertures (as is the case here), maximizing the field of view similarity results in positioning the cameras at different distances from the object, which in turn will degrade the quality of one of the two images. It is therefore preferable to privilege the individual image quality at the expense of a few tens of pixels that are eventually cropped out.

In this workflow, image registration is first performed coarsely with the scale-invariant feature transform (SIFT) [19] and then the learned transform is refined with the registration method introduced by Conover et al. [20].

Another fundamental alignment that should be aimed at, is that of the relative geometry between camera - light source - artifact. Achieving this feature in the experimental set-up is beneficial to the step of spectral splicing. Indeed, the amount of reflected light that is measured by a camera depends significantly on the angle of incidence of the light, the angle of the observed surface, and the angle of view of the camera (following a physical function called BRDF – Bidirectional Reflectance Distribution Function [21]). In a scenario in which these angles are adjusted manually, it is still possible to be prone to human errors. Small misalignments contribute, together with other sources of noise at the sensor level, to a mismatch in response values when we observe adjacent or overlapping bands of different sensors. More intuitively, let's consider the weaving structure of textiles. It is observable that shining a light at 45° generates a pattern of micro shadows. For the splicing correction to function more effectively, i.e. to produce realistic spectra, these shadows must be found in the same locations in the two scenes that are meant to be fused.

The application of sharpening techniques does not require further optimizations of the experimental setup but calls for caution when selecting the right algorithm. In the literature on sharpening methods, there exists a plethora of solutions, each based on different families of techniques. What is important to highlight, is that all methods have been developed for the domain of remote sensing, which is profoundly different from technical imaging for Cultural Heritage. Indeed, the extension of sharpening techniques to applications on historical artefacts is still an unexplored topic [22]. Remotely sensed images are usually characterized by urban, forest, and crop scenes that rarely change their spatial patterns when observed over a large spectral range spanning from visible to SWIR radiation.

On the other hand, textiles showcase dyestuff information in the visible range and fiber information in the SWIR range. This example is reported in Figure 4, where images in the visible and infrared ranges are compared for two different scenes: an urban landscape imaged by the APEX imaging spectrometer [23] and a modern dyed textile. It is evident how a change in spatial structures takes place as the dye information gets lost in the infrared images. If this feature of textiles is not carefully taken into account, the sharpening step may result in the production of

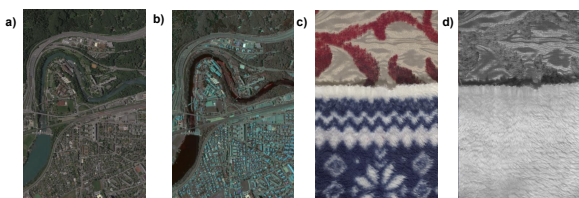


Figure 4. a) Remotely sensed image in the VNIR range captured by the APEX hyperspectral imager. b) Same scene in the SWIR range. c) VNIR image of a modern dyed textile captured with the system described in this article. d) Same scene in the SWIR range. This is an example of how spatial patterns are typically conserved when moving from a visible to an infrared representation in remotely sensed images. In textile imaging, this does not happen.

an image with artificially generated spatial details that can hinder the analysis. To show this effect, the sharpening step is performed with two methods coming from two traditional families of sharpening techniques [15]: Gram-Schmidt (GS - family of component substitution) and MTF-GLP-CBD (family of multi-resolution analysis). It will be demonstrated how the latter can better neglect spatial details that should not be injected, thus resulting in a more truthful classification of fibers. The spawning of *degenerated* spectral profiles via GS is a well-known effect in the remote sensing community. However, with this demonstration, we want to stress the importance of selecting the correct method for the particular application of SWIR sharpening from VNIR data in the context of archaeological textiles.

Results and Demonstrations

Image Registration

Given the size of the textile fragment and the adopted capturing distance, it was necessary to scan the artefact twice in order to image the whole surface. The two slices are reported in Figure 1b, and it is possible to observe that they share a significant overlap, which can be used to register the two parts and compose the image in Figure 1b. Table 1 reports the values of pixel displacement (Δp) and GSD error (ΔGSD) that are achieved when registering various image pairs at different scales of resolution. All registration processes achieve sub-pixel accuracy, which is a sign of a successful alignment step.

Table 1. Pixel displacement values for registration. HR: high resolution, LR: low resolution. Numbers 1 and 2 refer to the notation in Figure 1b, while V and S refer to VNIR and SWIR, respectively.

Resolution	Fixed	Moving	Δp	ΔGSD (μm)
HR	1V	2V	0.72	36
HR	1V	1S	0.72	36
HR	2V	2S	0.94	47
LR	1S	2S	0.35	70
LR	1S	1V	0.36	72
LR	2S	2V	0.39	78

When composing the full hyperspectral image from 400 to 2500 nm, the images of individual slices are registered together first, and then the *panorama* picture is composed.

Splicing

Spectral splicing aims to smoothly connect two hyperspectral sets. In the adopted method, the bands that are found close

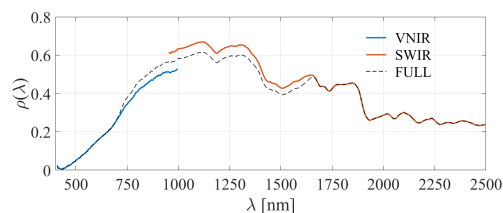


Figure 5. Spectral splicing example. The VNIR and SWIR spectra are merged into the FULL spectrum in a way that limits the overall intervention and preserves the shape of the expected resulting spectrum.

to the overlap region (950-1000 nm) are corrected more strongly than those that are further. Figure 5 displays how two sample VNIR and SWIR spectra are corrected. Notice how eventually the corrected spectrum matches the original VNIR and SWIR spectra as we observe data points away from the overlapping interval.

Sharpening

The task of enhancing the resolution of the SWIR hyperspectral image to match that of the VNIR hyperspectral image was conducted following the paradigms formulated by Selva et al. [16] when they introduced the concept of hypersharpening.

As already mentioned, there is no way, other than a visual inspection, to assess the performances of a spatial resolution enhancement process, since the ground truth is missing. For this reason, it was decided to quantify the performances of the two selected sharpening algorithms (GS and MTF-GLP-CBD) following Wald's protocol. Here, both VNIR and SWIR hyperspectral images were reduced in size so that the newly generated VNIR hyperspectral set matched the spatial dimensions of the originally captured SWIR set. In principle, by enhancing the resolution of the downgraded SWIR image, one should obtain the originally captured SWIR set. Table 2 reports the performances of the two algorithms for different evaluation metrics. The ideal values of the metrics are reported in the ground truth (GT) column. Spectral Angle (SA) is a metric that evaluates how similar two spectra are in their shape, so it gives an indication regarding spectral fidelity. The Peak Signal-to-Noise Ratio (PSNR) measures the similarity between two images and is often used as an image quality metric. The *relative dimensionless error in synthesis* (ERGAS) measures the global distortion from a reference multi-band image.

The values reported in Table 2 are generally good for both algorithms. However, there exists a significant edge towards the MTF-GLP-CBD method both in terms of spectral fidelity and image quality, whereas both algorithms introduce the same amount of distortions.

Table 2. Performance metrics computed at low resolution.

Algorithm	SA	PSNR	ERGAS
GT	0	∞	0
GS	0.049	27.19	18.78
MTF-GLP-CBD	0.027	30.	18.87

Having assessed that both algorithms produce high-quality results, the assumption that is consequently made is that they are scale-invariant so that they can be applied to enhance the resolution of the originally captured SWIR image.

Figure 6 shows a false color image of a detail of the textile fragment in three different conditions: at the originally captured

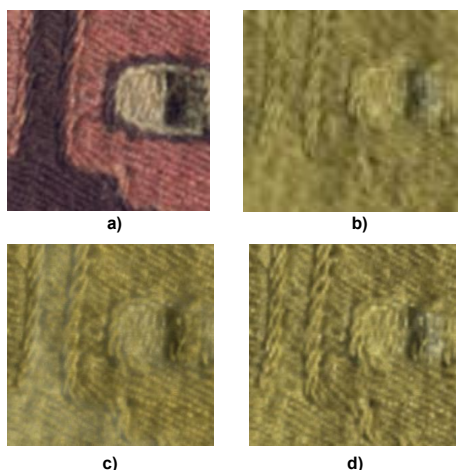


Figure 6. Detail of the textile fragment represented in color and infrared false color. **a)** Color image computed from VNIR data at high resolution. **b)** SWIR image as captured. **c)** Sharpening of SWIR with Gram-Schmidt. **d)** Sharpening of SWIR with MTF-GLP-CBD.

SWIR resolution, at the sharpened resolution with GS, and at the sharpened resolution with MTF-GLP-CBD. The false color is composed by selecting the following bands for the red, green, and blue channels respectively: 1644 nm, 1846 nm, 2228 nm.

As mentioned in the previous sections, some sharpening algorithms fail to correctly transfer the high spatial resolution information from the guiding image onto the image that is to be enhanced. This does not mean that the achieved spatial resolution is poor, but rather, it is possible that some spatial details are injected blindly, and thus can be thought as if they are false positives.

We demonstrate this effect by comparing a simple classification task on the sharpened images generated via GS and MTF-GLP-CBD. The demonstration is conducted at the lower resolution of the originally captured SWIR image, and thus the sharpened images are obtained via Wald's protocol.

From the scene, three relevant SWIR signals are extracted and compared to the spectra of each pixel by means of spectral correlation [24]. If the correlation is higher than 0.99, the pixel receives a label corresponding to one of the three signals, otherwise, it remains unclassified. Figure 7 depicts the classification maps. The ground truth image Figure 7a shows that various spatial structures do not pass the threshold check. The mapping is almost perfectly replicated in (7c), which reports the classification results obtained when applying MTF-GLP-CBD sharpening. On the other hand, it is very evident how GS sharpening produced a different result (7b). Here, the pixels that were originally unclassified, are now confidently labeled as Signal #3. This is a potentially dangerous result that sprouts from the fact that GS blindly injects spatial details from the guiding image and can then sometimes alter the spectral properties of entire areas.

Conclusion

The presented workflow provides a gateway to look into the possibilities that hyperspectral imaging in combined VNIR-SWIR ranges offers for the study of archaeological textiles. The focus of the article was mainly set to emphasize the important role that the experimental imaging setup covers, both in terms of artefact safety and expected data quality. In detail, we discussed the implications that an enhancing processing step such as sharpening can have on the interpretation of the hyperspectral data,

showing that selecting the inappropriate algorithm can at times lead to wrongly characterizing some areas of the textile.

Acknowledgments

The authors would like to express their gratitude to Lavinia de Ferri, Margunn Veseth, and Ralf Znotins of the Museum of Cultural History of the University of Oslo, for helping to access the collection and for their assistance in handling the textile fragments.

References

- [1] James M Adovasio and Thomas F Lynch. Preceramic textiles and cordage from Guitarrero Cave, Peru. *American Antiquity*, 38(1):84–90, 1973.
- [2] Pablo Prego Meleiro and Carmen García-Ruiz. Spectroscopic techniques for the forensic analysis of textile fibers. *Applied Spectroscopy Reviews*, 51(4):278–301, 2016.
- [3] Jinfeng Zhou, Lingjie Yu, Qian Ding, and Rongwu Wang. Textile fiber identification using near-infrared spectroscopy and pattern recognition. *Autex Research Journal*, 19(2):201–209, 2019.
- [4] Pilleriin Peets, Karl Kaupmees, Signe Vahur, and Ivo Leito. Reflectance FT-IR spectroscopy as a viable option for textile fiber identification. *Heritage Science*, 7(1):1–10, 2019.
- [5] Francesca Sabatini, Martina Bacigalupo, Ilaria Degano, Anna Javér, and Marei Hacke. Revealing the organic dye and mordant composition of paracas textiles by a combined analytical approach. *Heritage Science*, 8:1–17, 2020.
- [6] Jennifer Campos Ayala, Samantha Mahan, Brenan Wilson, Kay Antúnez de Mayolo, Kathryn Jakes, Renée Stein, and Ruth Ann Armitage. Characterizing the dyes of Pre-Columbian andean textiles: Comparison of ambient ionization mass spectrometry and HPLC-DAD. *Heritage*, 4(3):1639–1659, 2021.
- [7] Freddy Celis, Camilo Segura, Juan Sebastián Gómez-Jeria, Marcelo Campos-Vallette, and Santiago Sanchez-Cortes. Analysis of biomolecules in cochineal dyed archaeological textiles by surface-enhanced Raman spectroscopy. *Scientific Reports*, 11(1):1–11, 2021.
- [8] Li Ding, Tianyi Gong, Bo Wang, Qin Yang, Wei Liu, Rigzin Pemo, and Tsoky Metok. Non-invasive study of natural dyes in textiles of the Qing Dynasty using fiber optic reflectance spectroscopy. *Journal of Cultural Heritage*, 47:69–78, 2021.
- [9] Hengqian Zhao, Yunli Wang, Shuai Liu, Kunheng Li, and Wei Gao. Spectral reflectance characterization and fiber type discrimination for common natural textile materials using a portable spectroradiometer. *Journal of Archaeological Science*, 111:105026, 2019.
- [10] Roy S Berns. *Billmeyer and Saltzman's principles of color technology*. John Wiley & Sons, 2019.
- [11] John K Delaney, Paola Ricciardi, Lisha Glinsman, Michael Palmer, and Julia Burke. Use of near infrared reflectance imaging spectroscopy to map wool and silk fibres in historic tapestries. *Analytical Methods*, 8(44):7886–7890, 2016.
- [12] GM Atiqur Rahaman, Jussi Parkkinen, and Markku Hauta-Kasari. A novel approach to using spectral imaging to classify dyes in colored fibers. *Sensors*, 20(16):4379, 2020.
- [13] Arthur Ardeshtir Goshtasby. *2-D and 3-D image registration: for medical, remote sensing, and industrial applications*. John Wiley & Sons, 2005.
- [14] Federico Grillini, Jean-Baptiste Thomas, and Sony George. Logistic splicing correction for VNIR-SWIR reflectance imaging spectroscopy. *Optics Letters*, 48(2):403–406, 2023.
- [15] Gemine Vivone, Mauro Dalla Mura, Andrea Garzelli, Rocco Restaino, Giuseppe Scarpa, Magnus O Ulfarsson, Luciano Alparone, and Jocelyn Chanussot. A new benchmark based on re-

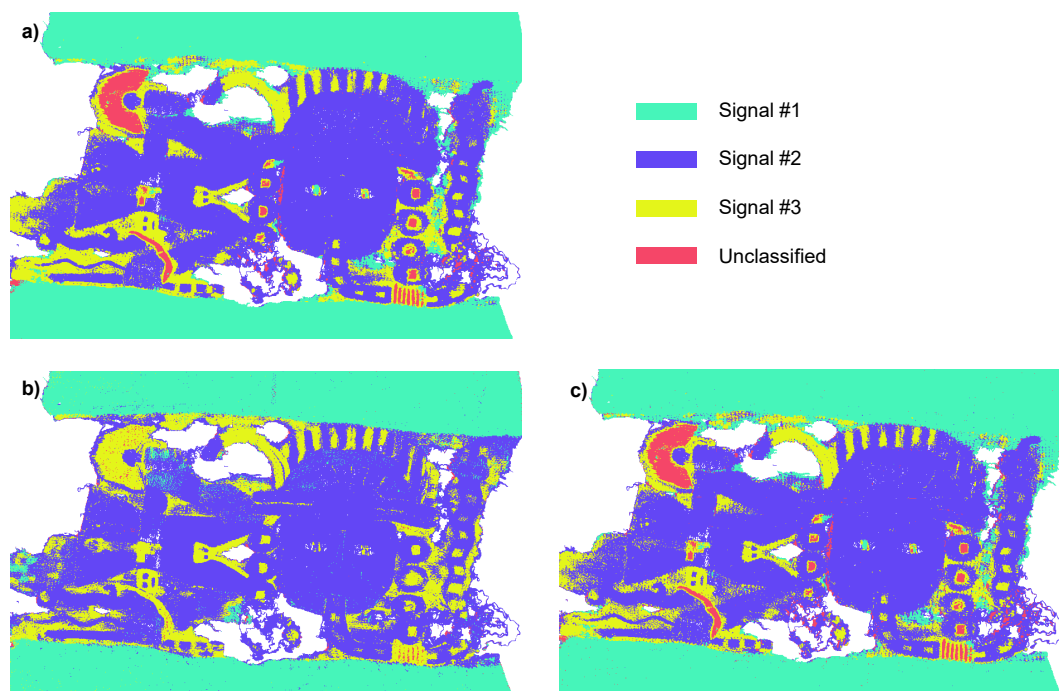


Figure 7. Mapping of three relevant SWIR signals. **a)** Original SWIR image as captured, which serves in this case as ground truth. **b)** SWIR image sharpened with Gram-Schmidt. **c)** SWIR image sharpened with MTF-GLP-CBD. Pixels that do not reach a satisfactory threshold for classification remain unlabeled. However, such pixels are classified when GS sharpening is applied and thus are false positive cases. MTF-GLP-CBD is able to correctly classify (or better not classify) them, since their spectral features remain unchanged.

cent advances in multispectral pansharpening: Revisiting pansharpening with classical and emerging pansharpening methods. *IEEE Geoscience and Remote Sensing Magazine*, 9(1):53–81, 2020.

- [16] Massimo Selva, Bruno Aiazzi, Francesco Butera, Leandro Chiarantini, and Stefano Baronti. Hyper-sharpening: A first approach on SIM-GA data. *IEEE Journal of selected topics in applied earth observations and remote sensing*, 8(6):3008–3024, 2015.
- [17] Lucien Wald. Quality of high resolution synthesised images: Is there a simple criterion? In *Third conference " Fusion of Earth data: merging point measurements, raster maps and remotely sensed images"*, pages 99–103. SEE/URISCA, 2000.
- [18] Roberto Padoan, Marvin E Klein, Roger M Groves, Gerrit de Bruin, Ted AG Steemers, and Matija Strlič. Quantitative assessment of impact and sensitivity of imaging spectroscopy for monitoring of ageing of archival documents. *Heritage*, 4(1):105–124, 2021.
- [19] David G Lowe. Distinctive image features from scale-invariant keypoints. *International journal of computer vision*, 60:91–110, 2004.
- [20] Damon M Conover, John K Delaney, and Murray H Loew. Automatic registration and mosaicking of technical images of Old Master paintings. *Applied Physics A*, 119:1567–1575, 2015.
- [21] Frederick O Bartell, Eustace L Dereniak, and William L Wolfe. The theory and measurement of bidirectional reflectance distribution function (BRDF) and bidirectional transmittance distribution function (BTDF). In *Radiation scattering in optical systems*, volume 257, pages 154–160. SPIE, 1981.
- [22] Tyler R Peery and David W Messinger. Panchromatic sharpening enabling low-intensity imaging of cultural heritage documents. In *Image Sensing Technologies: Materials, Devices, Systems, and Applications VI*, volume 10980, page 1098004. SPIE, 2019.
- [23] Michael E Schaepman, Michael Jehle, Andreas Hueni, Petra D’Odorico, Alexander Damm, Jürg Weyerermann, Fabian D Schneider, Valérie Laurent, Christoph Popp, Felix C Seidel, et al. Advanced radiometry measurements and earth science applications with the Airborne Prism Experiment (APEX). *Remote Sensing of*

Environment, 158:207–219, 2015.

- [24] O Abilio De Carvalho and Paulo Roberto Meneses. Spectral correlation mapper (SCM): an improvement on the spectral angle mapper (SAM). In *Summaries of the 9th JPL Airborne Earth Science Workshop, JPL Publication 00-18*, volume 9, page 2. JPL publication Pasadena, CA, USA, 2000.

Author Biography

Federico Grillini received his BSc degree in Optics and Optometry from the University of Florence (Italy) in 2017, and the MSc in Colour in Science and Industry from the joint Erasmus-Mundus program COSI (Universite Jean Monnet, Universidad de Granada, and NTNU) in 2020. Since the same year, he is a PhD candidate at the Norwegian Institute of Science and Technology (NTNU) in Gjøvik, Norway. His studies focus on hyperspectral imaging techniques for applications on cultural heritage.

Jean-Baptiste Thomas received his BSc in Applied Physics in 2004 and his MSc in Optics, Image and Vision in 2006, both from Université Jean Monnet in France. He received his PhD from Université de Bourgogne in 2009. Since 2010, he is Associate Professor at the Université de Bourgogne. Between 2016 and 2019 he was on a research leave at NTNU. Since 2019 he is Associate Professor at NTNU. He has worked extensively on the development of spectral imaging systems through Spectral Filter Arrays technology. Since 2016 he has worked on understanding material appearance and its measure by using imaging systems.

Sony George is currently Associate Professor at The Norwegian Colour and Visual Computing Laboratory, Norwegian University of Science and Technology (NTNU) since 2017. Before joining NTNU, he worked as a researcher at Gjøvik University College, Norway. Sony obtained a PhD in Photonics from the Cochin University of Science and Technology, India in 2012. His research interests are in the field of spectral imaging and its applications. He has been involved in several national and EU projects in different roles: EU MSCA-ITN projects: CHANGE, HiPerNav, COST action: COSCH, MultiForSee.